Contrasting NPQ dynamics and xanthophyll cycling in a motile and a non-motile intertidal benthic diatom

Lander Blommaert[1,4], Marie J. J. Huysman[1,2,3], Wim Vyverman[1], Johann Lavaud[4,5] & Koen Sabbe[1*]

1 Ghent University, Lab. Protistology & Aquatic Ecology, B-9000 Ghent, Belgium

2 VIB, Department of Plant Systems Biology, B-9052 Ghent, Belgium

3 Ghent University, Department of Plant Biotechnology and Bioinformatics, B-9052 Ghent, Belgium

4 CNRS/Université de La Rochelle, UMR7266 LIENSs, Institut du Littoral et de l'Environnement, 17000 La Rochelle, France

5 Current address : CNRS/Université Laval, UMI3376 Takuvik Joint International Laboratory, Département de Biologie, Pavillon Alexandre Vachon, Université Laval, 1045 avenue de la Médecine, Québec, Qc, G1V 0A6, Canada

* Corresponding author:

Ghent University, Lab. Protistology & Aquatic Ecology, Krijgslaan 281-S8 B-9000 Ghent, Belgium, Phone: +32-(0)9-264-85-11, E-mail: koen.sabbe@ugent.be

Running head : Photoprotection in intertidal diatoms

Keywords: photoprotection, xanthophyll cycle, microphytobenthos, diatom, non-photochemical quenching

Abstract

Diatoms living in intertidal sediments have to be able to rapidly adjust photosynthesis in response to often pronounced changes in light intensity during tidal cycles and changes in weather conditions. Strategies to deal with oversaturating light conditions, however, differ between growth forms. Motile epipelic diatoms can migrate to more optimal light conditions. In contrast, non-motile epipsammic diatoms appear to mainly rely on higher Non-Photochemical Quenching (NPQ) of chlorophyll *a* fluorescence to dissipate excess light energy, and this has been related to a larger pool of xanthophyll cycle (XC) pigments.

We studied the effect of 1 h high PAR (Photosynthetically Available Radiation) (2000 µmol photons m^{-2} s^{-1}) on the kinetics of the xanthophyll cycle and NPQ in both a motile diatom (*Seminavis robusta*) and a non-motile diatom (*Opephora guenter-grassii*) in an experimental set-up which did not allow for vertical migration. *O. guenter-grassii* could rapidly switch NPQ on and off by relying on fast XC kinetics. This species also demonstrated high de novo synthesis of xanthophylls within a relatively short period of time (1 h), including significant amounts of zeaxanthin, a feature not observed before in other diatoms. In contrast, *S. robusta* showed slower NPQ and associated XC kinetics, partly relying on NPQ conferred by de novo synthetized diatoxanthin molecules and synthesis of Light-Harvesting Complex X (LHCX) isoforms. Part of this observed NPQ increase, however, is sustained quenching (NPQs). Our data illustrate the high and diverse adaptive capacity of microalgal growth forms to maximize photosynthesis in dynamic light environments.

Introduction

Diatoms are dominant primary producers in areas characterized by pronounced fluctuations in light conditions (Armbrust 2009; Lavaud and Goss 2014). Rapid changes in light climate in well mixed waters or on intertidal flats challenge planktonic and benthic diatoms, respectively, to adjust light harvesting to what can be safely used for photosynthesis. As periods of high light conditions can result in oxidative damage to, in particular, the photosystem II (PSII) core, diatoms possess various mechanisms to deal with high light stress: (1) avoid excess light energy absorption by decreasing cell pigment content (MacIntyre et al. 2002); (2) dissipate excess excitation energy as heat in a process called Non-Photochemical Quenching of chlorophyll *a* (Chl *a*) fluorescence (NPQ) (Lavaud and Goss 2014; Goss and Lepetit 2015), and/or by engaging alternative electron cycling pathways (Wagner et al. 2016); (3) scavenge reactive oxygen species (ROS) (Janknegt et al. 2008, 2009a; b; Waring et al. 2010); (4) repair damaged PSII cores, mainly by replacing the D1 protein of the PSII reaction centre (Wu et al. 2011; Lavaud et al. 2016); (5) behavioural down regulation through vertical cell movement (microcycling and bulk migration) (Kromkamp et al. 1998; Serôdio 2004). Of the above mechanisms, especially NPQ is able to track fast light fluctuations experienced in the natural habitat (Brunet and Lavaud 2010; Lavaud and Goss 2014).

In land plants, three NPQ components have been distinguished, based on the relaxation kinetics after high light exposure: the rapidly relaxing component qE (seconds to minutes), the slower state transitions qT (tens of minutes), and the so-called 'photoinhibitory' quenching qI, which relaxes in the range of hours (Horton and Hague 1988). In diatoms, however, only two of these have been observed (Owens 1986). Energy dependent quenching (qE) is the main component and

70 is controlled by (1) the build-up of a proton gradient (ΔpH) across the thylakoid membrane, (2)
71 the (reversible) de-epoxidation of diadinoxanthin (Ddx) to diatoxanthin (Dtx) in the xanthophyll
72 cycle (XC) and (3) the presence of Light-Harvesting Complex X (LHCX) proteins, homologs of
73 the Light-Harvesting Complex Stress-Related (LHCSR) proteins found in green algae (Lavaud
74 and Goss 2014; Goss and Lepetit 2015). The origin of the second component (qI), however, is
75 less clear. Besides PSII photoinactivation and damage, Dtx and some LHCX isoforms might be
76 involved in this sustained quenching mechanism (Zhu and Green 2010; Lavaud and Lepetit
77 2013). It is increasingly referred to as NPQs (for sustained NPQ) or 'dark NPQ' as it persists
78 even under prolonged dark acclimation, particularly in intertidal benthic diatoms (Perkins et al.
79 2011; Lavaud and Goss 2014).
80
81 A molecular mechanism of qE in diatoms has been recently proposed (Lavaud and Goss 2014;
82 Goss and Lepetit 2015). qE is hypothesized to be based on two quenching sites within the LHC
83 antenna of PSII: 1) Q2 which is localized in a part of the LHC that remains attached to the PSII
84 and which directly depends on the synthesis and activation of Dtx, and 2) Q1 which is localized
85 in a part of the LHC that detaches from PSII upon Dtx activation at Q2 and which forms an
86 energy sink that amplifies Q2 quenching. It is believed that the persistence of Dtx, even in the
87 dark, is responsible for keeping both quenching sites active and especially Q1, i.e. as long as Dtx
88 is present at Q2 site, FCP (Fucoxanthin Chlorophyll *a*/*c* binding Protein) oligomers cannot
89 reconnect to PSII which generates part of the sustained qI/NPQs (Lavaud and Goss 2014).
90 Marked differences in NPQ capacity and kinetics were discovered between planktonic diatom
91 species and even between ecotypes isolated from habitats experiencing different degrees of
92 average irradiances and/or light fluctuations. These differences have been attributed either to
93 variation in XC kinetics and/or the amount of LHCX proteins (Lavaud et al. 2007; Dimier et al.

2007; Bailleul et al. 2010; Petrou et al. 2011; Lavaud and Lepetit 2013; Lepetit et al. *in press*). The emerging picture from these reports is that a higher/faster Dtx synthesis supports a faster NPQ induction and a higher NPQ capacity in species/ecotypes adapted to habitats characterized by strong light fluctuations and/or average higher irradiance (Lavaud and Goss 2014). One of the specificities is the de novo Dtx synthesis, which in case of prolonged stress light conditions helps to amplify photoprotection via enhanced NPQ and/or ROS scavenging (Lepetit et al. 2010). Species thriving in fluctuating light conditions, for example, exhibit high de novo synthesis of Dtx molecules which correlates well with NPQ development during strong light conditions. Species experiencing a more stable light climate in their natural habitat also synthetize Dtx molecules de novo when shifted to high light conditions but these are probably not involved in NPQ but may rather have an antioxidant function (Lavaud and Lepetit 2013). In addition to a high NPQ capacity and fast Dtx production during oversaturating light conditions, fast relaxation of NPQ in low light conditions is key to track changes in irradiance (Lavaud et al. 2007). As Dtx molecules have to be epoxidized back to Ddx to switch the antenna system from an energy dissipating to a light harvesting mode, diatoms with a high Dtx epoxidation rate dissipate NPQ faster compared to diatoms with a lower epoxidation rate (Goss et al. 2006; Goss and Jakob 2010). A difference in NPQ capacity can also be attributed to differences in LHCX protein content. The low amount of LHCX1 protein, for instance, explains limited NPQ capacity in a high latitude *Phaeodactylum tricornutum* ecotype isolated from a supralitoral rockpool (P.t.4) which experiences lower average light intensity, and less drastically fluctuating light conditions, compared to other ecotypes (Bailleul et al. 2010). Whereas the *LHCX1* gene is already maximally expressed in low light conditions, several other *LHCX* family members of both centric and pennate diatoms are highly and rapidly upregulated when exposed to high light (Nymark et al. 2009; Park et al. 2010; Zhu and Green 2010; Lepetit et al. 2013, *in press*) and other stressful

environmental conditions that impair photosynthetic capacity (Taddei et al. 2016). These proteins might either confer higher NPQ capacity by binding newly synthetized Dtx molecules and/or be involved in NPQs after prolonged high light exposure (Zhu and Green 2010; Lepetit et al. 2013, *in press*).

While our knowledge of NPQ regulation is mostly based on studies of planktonic diatoms, whose light climate is mostly governed by water column turbulence, far less attention has been paid to NPQ regulation in benthic diatoms thriving in, and on, the sediments of intertidal flats (Jesus et al. 2009; Perkins et al. 2010; Cartaxana et al. 2011, 2016a; b; Serôdio et al. 2012; Lavaud and Goss 2014; Ezequiel et al. 2015; Pniewski et al. 2015; Laviale et al. 2015). Like terrestrial plants, these diatoms can experience fast light fluctuations, not buffered by a water column, during low tide. The tidal rhythm, furthermore, can change the light climate drastically as no or very little light reaches the sediments in turbid estuaries when submerged (Underwood and Kromkamp 1999).

NPQ capacity of intertidal benthic diatoms is mainly defined by their ability or inability to avoid excess light energy (Jesus et al. 2009; Cartaxana et al. 2011; Barnett et al. 2015). Diatoms belonging to the raphid clade possess a raphe system that allows movement by secreting extracellular polymer substances (EPS) through the raphe slit. Raphid diatoms can thus migrate vertically into the sediment matrix to a more optimal light climate (Consalvey et al. 2004). In addition, microcycling of motile diatoms within the top layers of the sediments was proposed with algae migrating down to avoid photoinhibition being replaced by others (Kromkamp et al. 1998; Serôdio 2004). Such sequential turnover at the species level was indeed observed in

141 laboratory mesocosms (Paterson 1986) and during an in situ emersion period (Underwood et al.
142 2005).
143
144 In contrast, diatoms living attached or in close association with single sand grains (epipsammic
145 diatoms) are immotile or only capable of limited movement and therefore need to rely on
146 physiological photoprotection (Cartaxana et al. 2011). This can explain a higher deepoxidation of
147 the Ddx-Dtx cycle pigments in epipsammic communities (Jesus et al. 2009). Barnett et al. (2015)
148 experimentally demonstrated higher NPQ values, coupled with higher Dtx content, in
149 epipsammic diatoms. A more comprehensive comparison between the regulation and kinetics of
150 the NPQ mechanism of both motile and non-motile diatoms, however, has so far not been made.
151 In this study we demonstrate fast irradiance tuning of NPQ, coupled with fast XC kinetics in the
152 immotile epipsammic diatom species *Opephora guenter-grassii*. We show that this species, in
153 addition to Dtx, also accumulates considerable amounts of the de-epoxidized xanthophyll
154 zeaxanthin (Zx) during a short period (1 h) of high light exposure, a feature so far only observed
155 in planktonic diatoms after prolonged (up to 6 h) periods of oversaturating light conditions (Lohr
156 and Wilhelm 1999). As the high de novo synthesis of de-epoxidized xanthophylls in this species
157 is not paralleled by an equal increase in NPQ, these xanthophylls are not expected to be directly
158 involved in the NPQ mechanism. In contrast, an epipelic species, *Seminavis robusta*, shows a less
159 dynamic NPQ, despite concerted de novo synthesis of both Dtx molecules and LHCX proteins.
160 Our findings add to the physiological underpinning of the differential response of motile and non-
161 motile diatom species (Juneau et al. 2015; Barnett et al. 2015) and of benthic diatom communities
162 in sediment (Pniewski et al. 2015; Laviale et al. 2015; Cartaxana et al. 2016b) to their
163 environment.
164

Materials

Culture conditions

Strains were obtained from the diatom culture collection (BCCM/DCG) of the Belgian Coordinated Collection of Micro-organisms (http://bccm.belspo.be), accession numbers *Seminavis robusta* (DCG 0105) and *Opephora guenter-grassii* (DCG 0448), and grown in semi-continuous batch culture in 1.8 l glass Fernbach flasks (Schott) in a day/night rhythm of 16/8 hour with a Photosynthetically Available Radiation (PAR) of 20 µmol photons m^{-2} s^{-1}. Cells were cultured in Provasoli's enriched f/2 seawater medium using Tropic Marin artificial sea salt (34.5 g l^{-1}) enriched with $NaHCO_3$ (80 mg l^{-1} final concentration). Cultures were acclimated to these culturing conditions for at least 2 weeks. Chlorophyll *a* (Chl *a*) was measured daily according to Jeffrey & Humphrey (1975) to monitor growth.

High light exposure

Cultures in exponential growth were concentrated to 10 mg Chl *a* l^{-1} by centrifugation (Eppendorf 5810 R) at 4000 RCF for 5 min in 50 ml falcons. The cultures were again acclimated to their growth conditions for 2 h before exposure to high light. Immediately before the experiment started $NaHCO_3$ (4 mM, final concentration) was added from a 2 M stock to prevent carbon limitation during the experiment. Four 65 W white light energy-saving lamps (Lexman) were used to provide high light (HL) conditions (2000 µmol photons m^{-2} s^{-1}) for one hour. Cells were then allowed to recover for one hour in low light (LL, 20 µmol photons m^{-2} s^{-1}), provided by one 20 W Lexman energy saving lamp. All light conditions were measured as PAR with a spherical micro quantum sensor (Walz) submerged in the centre of a 10 mg Chl *a* l^{-1} diatom suspension, thus corresponding to the concentrations used during the experiments. Cells were

188 continuously stirred in a glass test tube to obtain a homogenous cell suspension. This glass test
189 tube was cooled in a custom-made glass cooler by a water bath at 20°C.
190
191 **LHCX protein detection**
192 Sampling was conducted as described by Lepetit et al. (2013). Samples were taken immediately
193 before light exposure (T0), after one hour HL and after one subsequent hour of LL recovery.
194 Protein extraction, SDS-PAGE, Western-blot and ECL immunodetection were carried out as
195 published by Laviale et al. (2015). Both an FCP6 antibody (dilution 1/10000), Anti-FCP6
196 (LHCX1) from *Cyclotella cryptica* (Westermann and Rhiel 2005), and an anti-LHCSR3 (dilution
197 1/20000) from *Chlamydomonas reinhardtii* (Bonente et al. 2011) were tested. Anti-PsbB (CP47,
198 Agrisera) was used as a loading control. Anti-LHCX6 from *T. pseudonana* (Zhu and Green 2010)
199 was not usable for the two investigated species. *Phaeodactylum tricornutum* CCAP 1055/1 (P.t.)
200 samples exposed to HL for 3 hours were analysed at the same time as a control.
201
202 **Pigment analyses**
203 Diatom suspensions were rapidly filtered onto Isopore 1.2 µm RTTP filters (Merck Millipore),
204 immediately frozen in liquid nitrogen and stored at -80°C. Samples were freeze-dried before
205 adding -20°C cold 1.4 ml extraction buffer (90% methanol/0.2 M ammonium acetate (90/10
206 vol/vol) and 10% ethyl acetate). Pigment extraction was enhanced by adding glass beads
207 (diameter 0.25–0.5 mm, Roth) and vortexing for 30 s. The extracts were sonicated for 30 s on ice
208 at 40% amplitude with 2 s pulse, 1 s rest and filtered over a 0.2 µm filter. One hundred µl were
209 immediately injected into the HPLC system (Agilent). Samples were analysed according to Van
210 Heukelem and Thomas (2001). As buffered extraction medium was used, no additional TBAA

buffer was injected. All pigment concentrations (chlorophyll *c* (Chl *c*), fucoxanthin (Fx), diadinoxanthin (Ddx), diatoxanthin (Dtx), violaxanthin (Vx), antheraxanthin (Ax), zeaxanthin (Zx), chlorophyll *a* (Chl *a*) and *β*-carotene (*β*-car)) were calculated by comparison with pigment standards. All standards were obtained from DHI, with exception of Chl *a* which was obtained from Sigma-Aldrich.

Pulse Amplitude Modulated (PAM) Fluorometry

Chlorophyll fluorescence was measured using a Diving PAM fluorometer (Walz). Saturating flashes (0.4 s, 3600 µmol photons $m^{-2}s^{-1}$) were provided by the internal halogen lamp to measure photosynthetic parameters (see Barnett et al. 2015 for a complete overview of parameters). The duration of 0.4 s for saturating pulses was tested as the best setting for measurement of the maximum photosynthetic efficiency of PSII (F_v/F_m) and effective quantum efficiency of PSII photochemistry ($\Delta F/F_m'$). When applied longer, the maximal fluorescence yield (F_m) is under-estimated which artificially lowers F_v/F_m and $\Delta F/F_m'$. This is most probably due to the high energy delivered by the halogen lamp of the Diving-PAM fluorometer (different from the LEDs used for most other PAM fluorometers). We have applied these settings before (see Barnett et al. 2015) and it provided reliable results. To avoid interference from the HL setup, the lights were switched off immediately before firing a saturating pulse (see Lepetit et al. 2013). The photosynthetic efficiency of PSII ($\Delta F/F_m'$) was calculated as $(F_m'-F')/F_m'$ and expressed as a percentage, taking the maximal photosynthetic efficiency (F_v/F_m), measured immediately before HL onset as 100%. Non-Photochemical Quenching (NPQ) was calculated as $(F_m-F_m')/F_m'$.

Rate estimation and statistics

The $\Delta F/F_m$' recovery rate constant (k) was calculated by fitting an exponential decay function:

$$\Delta F/F_m'(t) = \Delta F/F_m'rec + [\Delta F/F_m'(0) - \Delta F/F_m'rec]e^{-kt}$$

where t represents time (in min) during recovery and $\Delta F/F_m'(0)$ and $\Delta F/F_m'rec$ represents $\Delta F/F_m'$ (expressed in percentage from the $\Delta F/F_m'$ before HL onset) at the start of the recovery period and after 30 min of recovery in LL respectively (Serôdio et al. 2012). Ddx de-epoxidation, Dtx and Zx epoxidation and the XC de novo synthesis rates were calculated as in Lavaud et al. (2004) using exponential decay functions for epoxidation and de-epoxidation rate constants (k). The Ddx epoxidation, for instance, was fitted as the decrease of Ddx with the exponential decay function:

$$Ddx\ (t) = Ddx_{minimal} + (Ddx_{initial} - Ddx_{minimal})e^{-kt}$$

where t represents time (in min), and $Ddx_{initial}$ and $Ddx_{minimal}$ represent the highest and lowest observed concentrations, respectively. Linear functions were fitted for xanthophyll de novo synthesis rates. Statistical analyses were conducted using the statistical software package SAS 9.4. Species parameters (3 replicates per species) were compared using the general linear model PROC GLM. In case of unequal variances, a Welch's t-test was performed.

Results

General characteristics

The epipelic diatom *Seminavis robusta* and epipsammic diatom *Opephora guenter-grassii* were grown under low light (LL) conditions; resulting in a XC pigment pool (Ddx + Dtx) of 4.94 ± 0.45 mol (100 mol Chl *a*)$^{-1}$ for *S. robusta* and 9.88 ± 0.59 mol (100 mol Chl *a*)$^{-1}$ for *O. guenter-grassii*. The maximal PSII quantum yield $\Delta F/F_m$, measured immediately before HL exposure and without dark adaptation, was 0.685 ± 0.031 for *S. robusta* and 0.665 ± 0.017 for *O. guenter-grassii* and did not differ significantly ($p = 0.099$) between the two species. This indicates that the cells were in an unstressed condition prior to HL exposure, which is also supported by the absence or negligible concentrations of diatoxanthin (Dtx).

PSII quantum yield and NPQ

Both *O. guenter-grassii* and *S. robusta* were exposed to HL for one hour, after which they were allowed to recover in LL conditions. The quantum yield of PSII ($\Delta F/F_m$') of both species dropped during HL (Fig. 1a), but was significantly higher for *O. guenter-grassii* at the end of the HL period in comparison with *S. robusta* ($p = 0.049$, Welch-test). During the subsequent low light conditions $\Delta F/F_m$' of *O. guenter-grassii* recovered about 90 % of its value before HL exposure whereas *S. robusta* recovered less than 75 %. The $\Delta F/F_m$' recovery rate constant was more than double the rate constant for the epipsammic species (0.096 min^{-1} ± 0.009 compared to 0.040 min^{-1} ± 0.004 for *S. robusta*). At each time point during HL, NPQ was higher in *O. guenter-grassii,* compared to *S. robusta* (Fig. 1b). During the start of the LL period, *O. guenter-grassii* showed very rapid NPQ relaxation, with about half of its NPQ relaxing within 2.5 minutes. Both fast NPQ relaxation and recovery of $\Delta F/F_m$' slowed down when *O. guenter-grassii* was placed in darkness instead of LL (Fig. 2a&b). NPQ dissipation in *S. robusta* occurred more gradually and

was incomplete after one hour of LL, with a remaining NPQ of 0.504 ± 0.07 compared to 0.188 ± 0.002 for *O. guenter-grassii*.

Xanthophyll cycle characteristics

The higher Ddx-Dtx pool of *O. guenter-grassii* ($p = 0.000$) resulted in higher Dtx concentrations after 5 minutes of HL ($p = 0.0447$) (Fig. 3a&b, Table 1). The de-epoxidation state (DES, calculated as Dtx/(Ddx + Dtx)), however, was not significantly different between the species during the HL period (Fig. 4). From 15 minutes onwards the total Ddx + Dtx pool increased (due to de novo synthesis of xanthophylls) with similar rates in both species (Fig. 3a&b, Table 1). During one hour of HL treatment each species synthetized an additional 2 mol Ddx + Dtx (100 mol Chl a)$^{-1}$. At the end of the HL period *O. guenter-grassii* contained significantly ($p = 0.040$) more Dtx (5.69 ± 1.41 mol (100 mol Chl a)$^{-1}$) than *S. robusta* (3.15 ± 0.42 mol (100 mol Chl a)$^{-1}$) (Table 1). Due to the lower amount of Dtx originating from de-epoxidation of Ddx in *S. robusta* and similar de novo Dtx synthesis as *O. guenter-grassii*, the relative contribution of de novo synthetized Dtx was about two-thirds of the accumulated Dtx in *S. robusta*, whereas the de novo contribution was only one third in the case of *O. guenter-grassii*.

During the LL recovery period, Dtx was rapidly epoxidized by *O. guenter-grassii*. Its Dtx epoxidation rate constant in LL was about 5 times higher than in *S. robusta* ($p = 0.003$) (see Table 1), with most Dtx being epoxidized to Ddx within the first 5 min of LL recovery. Epoxidation occurred more gradually in *S. robusta* (Fig. 3a&b). Differences in epoxidation rate resulted in significant differences in de-epoxidation state at 5 ($p = 0.022$) and 15 min ($p = 0.019$) during the LL recovery period (Fig. 4). At the end of the recovery period however, nearly all Dtx had disappeared in both species (Fig. 3a&b, Table 1). The fast Dtx epoxidation by *O. guenter-*

295 *grassii* in LL was not observed in darkness (Fig. 2c). In both species, an increase in the Ddx +
296 Dtx pool was recorded during LL treatment. *O. guenter-grassii* gained 2.26 ± 0.21 mol Ddx +
297 Dtx (100 mol Chl *a*)$^{-1}$, whereas in *S. robusta* the increase was 1.84 ± 1.10 mol Ddx + Dtx (100
298 mol Chl *a*)$^{-1}$ (Table 1).
299 Besides the Dtx cycle pigments, pigments of the violaxanthin (Vx) cycle were detected in both
300 species during HL (Fig. 3c&d, Table 1). *O. guenter-grassii* accumulated about 2 mol (100 mol
301 Chl *a*)$^{-1}$ Vx cycle pigments during the HL period (Table 1). At the end of the HL treatment, 1.34
302 ± 0.19 mol (100 mol Chl *a*)$^{-1}$ of the de-epoxidized pigment Zeaxanthin (Zx) was detected in *O.*
303 *guenter-grassii*. The intermediate between Zx and Vx, antheraxanthin (Ax), was also detected
304 during HL (Fig. 3c). In comparison, *S. robusta* accumulated significantly less ($p = 0.001$) Vx
305 cycle pigments (Fig. 3d) and both Zx and Ax were only present in trace amounts. During the LL
306 recovery period epoxidation of Zx started immediately in *O. guenter-grassii*, resulting in a short
307 peak of Ax (at time point 2.5-5 min) and an increase in Vx. The total Vx cycle pool (Vx + Ax +
308 Zx) decreased markedly for both species during LL with a decrease of 1.62 ± 0.48 mol (100 mol
309 Chl *a*)$^{-1}$ for *O. guenter-grassii* and a smaller decrease of 0.07 ± 0.02 mol (100 mol Chl *a*)$^{-1}$ for *S.*
310 *robusta*. Notably, in *O. guenter-grassii*, Vx cycle pigments decreased as fast during the LL
311 period as new Ddx cycle pigments were synthetized (0.28 mmol (mol Chl *a*)$^{-1}$ min^{-1} ± 0.08 and
312 0.36 mmol (mol Chl *a*)$^{-1}$ min^{-1} ± 0.05 respectively). During the course of the experiment no
313 notable changes in Fx, Chl *c* and *β*-car were observed (Data not shown).
314
315 **Correlation between Dtx accumulation and NPQ**
316 NPQ correlated well with Dtx mol (100 mol Chl *a*)$^{-1}$ for both species (Fig. 5). They showed
317 similar slopes (0.7-0.8) until about 3 Dtx mol (100 mol Chl *a*)$^{-1}$, after which less NPQ was
318 developed per mol Dtx for *O. guenter-grassii*. The relationship remained true for *S. robusta*

during the course of the experiment. Its Dtx content, nevertheless, did not exceed the threshold at which the curve slope changed in *O. guenter-grassii*. The y-axis intercept differed from zero for *S. robusta*, as was reported earlier (Barnett et al. 2015).

LHCX presence during HL

For immunodetection of LHCX-isoforms in *O. guenter-grassii* (Fig. 6a) the best results were obtained using the anti-FCP6 antibody, as less a-specific binding occurred in comparison with the LHCSR3 antibody. Only one LHCX isoform could be detected with a molecular weight close to that of *Phaeodactylum tricornutum* LHCX3 (22.24 KDa). This isoform was apparent in LL acclimated cells and increased in abundance during the one hour of HL and the subsequent hour of recovery in LL.

In *S. robusta* (Fig. 6b) only the anti-LHCSR3 antibody revealed LHCX isoforms. One isoform, with a molecular weight equal to *P. tricornutum* LHCX3 (22.24 KDa) and another more faint band with an equal size to *P. tricornutum* LHCX2 (24.73 KDa) were present in LL acclimated cells. The former increased in abundance during HL and subsequent recovery in LL. After one hour of HL, moreover, two additional LHCX isoforms could be detected. An LHCX isoform of about 23 KDa was clearly present after one hour of HL and after the additional recovery period. The second one, about the size of LHCX1 in *P. tricornutum* (21.95 KDa), became visible after one hour of HL.

Discussion

In this study we demonstrate marked differences in irradiance tuning of NPQ and associated XC pigment and LHCX protein dynamics between a motile and a non-motile marine benthic diatom. The non-motile species (*O. guenter-grassii*) exhibits a dynamic and strong high-energy quenching (qE), coupled to fast XC kinetics and pronounced synthesis of de-epoxidized xanthophylls, including zeaxanthin. In this species, strong physiological photoprotection may compensate for its lack of motility as a way to avoid oversaturating light conditions. The motile species (*S. robusta*) on the other hand exhibited an overall lower qE capacity, even though NPQ increased during the light period, possibly due to de novo synthesis of both Dtx and LHCX proteins.

Prior to the experiments, both species were acclimated to low light conditions, to avoid the presence of Dtx and NPQ in cultures, as much as possible, which could bias the measurement of F_m. These growth conditions resulted in similar XC content as observed by Barnett et al. (2015) under identical light conditions for the same benthic species used in this study, and also as observed for a range of planktonic species grown in a PAR of 40 µmol photons $m^{-2}s^{-1}$ (Lavaud et al. 2004). The non-motile epipsammic species *O. guenter-grassii* showed higher NPQ during high light exposure, compared to the epipelic diatom *S. robusta*. As reported by Barnett et al. (2015), higher NPQ values coincided with a higher overall Dtx content de-epoxidized from a larger initial Ddx pool, rather than a higher de-epoxidation state (DES) or a higher involvement of Dtx molecules in the NPQ mechanism (Lavaud and Lepetit 2013). Indeed, we did not observe a difference in DES between *O. guenter-grassii* and *S. robusta*, nor a difference in the slopes of the NPQ/Dtx plots. Note that Jesus et al. (2009), working on natural epipelic and epipsammic

communities, did observe a difference in DES between both, but this may have been due to high light avoidance by vertical migration and/or microcycling in the epipelic communities, which was impeded in our study.

Accumulation of Dtx, independent from Ddx de-epoxidation, was observed for both species during high light exposure as reported for planktonic diatoms (Lavaud et al. 2004; Lavaud and Lepetit 2013) and natural epipelic communities (Laviale et al. 2015). The rate constant of this de novo Dtx synthesis was similar for both species and in the range of planktonic diatoms exposed to the same HL conditions (Lavaud et al. 2004), resulting in the same increase of the Ddx + Dtx pool. The XC pool at the end of the HL period, nonetheless, was still relatively low for both species, as up to 26 mol Ddx + Dtx (100 mol Chl *a*)$^{-1}$ were observed by Lohr and Wilhelm (1999) in *Cyclotella meneghiniana* and even up to 30-40 Ddx + Dtx (100 mol Chl *a*)$^{-1}$ in *Chaetoceros socialis* (Dimier et al. 2007). These large XC pools, however, required a prolonged exposure (i.e., several hours) to high irradiances, whereas in this study the HL period was relatively short (1 h). In the diatoms *Plagiogramma staurophorum* and *Brockmanniella brockmannii*, nonetheless, acclimation to a PAR of 75 µmol photons m^{-2}s^{-1} resulted in XC pools higher than 25 Ddx + Dtx (100 mol Chl *a*)$^{-1}$ (Barnett et al. 2015).

The involvement of de novo synthetized Dtx differed between both species. Whereas the NPQ-Dtx relationship remained true for *S. robusta*, de novo synthetized Dtx in *O. guenter-grassii* did not contribute equally to the NPQ mechanism, as shown by a decline in the NPQ-Dtx relationship. Part of this additionally synthetized Dtx is possibly present in the lipid matrix of the thylakoid membrane (Schumann et al. 2007) to prevent lipid peroxidation (Lepetit et al. 2010). It should be noted, however, that the total Dtx values observed for *S. robusta* during our experiments remained rather low compared to values recorded for other species using a similar setup (Lavaud et al. 2004; Lepetit et al. 2013; Lavaud and Lepetit 2013) and might be due to a

387 small Ddx pool before HL onset (Lavaud et al. 2004). A stable NPQ/Dtx slope during de novo
388 synthesis of Dtx, as observed in *S. robusta*, nonetheless, may indicate synthesis of new Dtx-
389 binding proteins such as LHCXs (Lepetit et al. 2013).
390 As fast epoxidation of Dtx is crucial to switch the light harvesting system from an energy
391 dissipation state to a light harvesting state, we monitored NPQ relaxation and Dtx epoxidation
392 during low light following high light exposure. *O. guenter-grassii* displayed very rapid Dtx
393 epoxidation coupled with an equally fast NPQ relaxation, but not during dark recovery, as
394 previously reported (Goss et al. 2006b). This is also demonstrated by the fast recovery of PSII
395 quantum yield in low light, which is severely restricted in darkness as the epoxidation reaction is
396 possibly slowed down by NADPH depletion (Goss et al. 2006b). The fast reversal of NPQ and
397 nearly complete recovery of PSII quantum yield, moreover, indicate that the observed high NPQ
398 values comprise mostly qE while qI/NPQs is virtually absent.
399 A fast switch from energy dissipation to light harvesting after high light exposure was not
400 observed in the epipelic diatom *S. robusta*, where Dtx epoxidation and coupled NPQ relaxation
401 occurred more gradually. Together with an incomplete and slower recovery of PSII quantum
402 yield our data demonstrate a higher susceptibility to photoinhibition during prolonged high light
403 as has been shown for species isolated from habitats lacking strong light fluctuations (Goss et al.
404 2006b; Su et al. 2012; Lavaud and Lepetit 2013). The observed NPQ values, increasing during
405 the high light treatment, therefore comprise not only qE but also a significant fraction of qI due to
406 PSII photoinactivation and damage (since Dtx is almost fully converted back to Ddx).
407 Even though both *S. robusta* and *O. guenter-grassii* accumulated similar amounts of newly
408 synthetized Dtx within one hour of high light, the latter synthetized the same amount of Vx cycle
409 and Dtx cycle pigments, including Zx. The presence of a parallel Vx-Ax-Zx cycle has been
410 demonstrated in several algae possessing the Ddx-Dtx cycle, including the diatom species

411 *Cyclotella meneghiniana* and *Phaeodactylum tricornutum* (Lohr & Wilhelm, 1999). Zx
412 accumulation in these species, however, required prolonged (up to 6 hours) high light exposure
413 (Lohr and Wilhelm 1999, 2001) and has never been reported in studies on *P. tricornutum* using
414 similar PAR and exposure time (i.e. within one hour, 2000 µmol photons $m^{-2}s^{-1}$) as used in this
415 study (Lavaud et al. 2004; Domingues et al. 2012; Lepetit et al. 2013; Lavaud and Lepetit 2013).
416 Epoxidation of Zx in low light was as fast as Dtx epoxidation, while the second epoxidation step
417 occurred more slowly, resulting in a transient peak in the intermediate Ax. This transient peak in
418 Ax has been reported before for the green alga *Chlorella* (Goss et al. 2006a). The Vx cycle pool
419 of *O. guenter-grassii* declined during the one hour recovery period and to a lesser degree also in
420 *S. robusta*, whereas a similar Vx cycle pool decline in *P. tricornutum* was not observed within
421 one hour of low light recovery (Lohr & Wilhelm, 1999). The high amount of Vx cycle pigments
422 synthetized by *O. guenter-grassii* in high light may have been converted to Ddx during the
423 recovery period, as the decline in Vx cycle pigments was paralleled by an equal increase in Ddx
424 + Dtx. A pathway from Vx to Ddx through the intermediate neoxanthin has been proposed by
425 Dambek et al. (2012). In *S. robusta*, however, more Ddx + Dtx accumulated during the LL period
426 than was lost from the Vx cycle pool. This might be due to additional synthesis of Ddx cycle
427 pigments during low light, even though additional de novo synthesis in low light conditions is
428 considered to be low (Lohr & Wilhelm, 1999). According to Lohr and Wilhelm (1999, 2001), the
429 primary role of Vx cycle pigments in diatoms is not photoprotection as they mainly serve as
430 intermediates in Ddx and fucoxanthin production. Increasing the light intensity, nonetheless,
431 changes the allocation of newly synthesized xanthophylls to the Vx-Ax-Zx pool in *P. tricornutum*
432 (Lohr and Wilhelm 1999). Moreover, Vx cycle pigments are mostly detected in algae displaying
433 high de novo xanthophyll synthesis combined with high de-epoxidase activity. This fits with our
434 observations of *O. guenter-grassii*, de novo synthetizing substantially more xanthophylls

435 (considering both Ddx and Zx cycle pigments) and de-epoxidising more Ddx to Dtx during HL
436 than *S. robusta*. We do not expect Zx to be directly involved in the NPQ mechanism of *O.*
437 *guenter-grassii* as the NPQ/Dtx relationship decreased during de novo synthesis of both
438 xanthophylls. In higher plants, Zx can dissolve in the thylakoid membrane lipids instead of being
439 protein bound (Jahns et al. 2009), scavenging reactive oxygen species with a higher capacity than
440 other xanthophylls found in higher plants (Havaux et al. 2007), or possibly regulating membrane
441 fluidity (Havaux and Gruszecki 1993).
442 As LHCX proteins play a central role in the NPQ mechanism of diatoms (Bailleul et al. 2010;
443 Zhu and Green 2010; Lepetit et al. 2013), we compared LHCX synthesis for the first time
444 between an epipsammic and an epipelic diatom. We could detect only one LHCX isoform (~22
445 kDa) in the epipsammic model *O. guenter-grassii* using the FCP6 antibody. It did not strongly
446 react to a shift to high light and was more abundant in subsequent low light. The epipelic diatom
447 *S. robusta*, however, revealed two out of four isoforms which strongly reacted to HL: one
448 isoform with MW ~23 kDa and a second one with MW ~19 kDa. Interestingly, in epipelic
449 communities, a 23 kDa isoform was shown to positively reacts to high light, high temperature
450 and motility inhibition (Laviale et al. 2015). The two isoforms already present in low light might
451 provide benthic diatoms with a basic NPQ to rapidly cope with sudden changes in light climate,
452 as has been demonstrated for LHCX1 of *P. tricornutum* (Bailleul et al., 2010). However, the *S.*
453 *robusta* genome does not contain a close homolog to the *P. tricornutum LHCX1* gene at the
454 sequence level (L. Blommaert et al., data not shown). LHCXs which are strongly upregulated
455 during high light have been suspected to either bind de novo synthetized Dtx, conferring higher
456 NPQ and/or participate in a sustained component of NPQ (NPQs) after prolonged high light
457 exposure (Zhu and Green 2010; Lepetit et al. 2013, *in press*). As *S. robusta* accumulates novel
458 Dtx during HL while its NPQ increases, the two observed light-responsive LHCX isoforms may

459 be responsible for Dtx binding, as suggested by Zhu and Green (2010), and Lepetit et al. (2013,
460 *in press*). However, other FCP proteins may be responsible as for instance the *LHCR6* and
461 *LHCR8* (Light-Harvesting Complex Red lineage) genes are strongly upregulated in *P.*
462 *tricornutum*, upon a shift to high light (Nymark et al. 2009).
463
464 **Ecological implications**

465 A fast and strong irradiance-tuning of NPQ is to be expected in immotile epipsammic diatoms as
466 they live attached to sand grains (Ribeiro et al. 2013) and are unable to move away from
467 oversaturating light conditions. Furthermore, sandy sediments are characterized by strong light
468 scattering in the uppermost layers, thereby increasing the average incident irradiance to which these
469 diatoms are exposed (Kuhl et al. 1994; Cartaxana et al. 2016b). Even though our epipsammic
470 species was acclimated to low PAR (20 µmol photons $m^{-2}s^{-1}$) it was able to cope with a sudden
471 change to a light intensity similar to full sunlight. Similar transitions from low to full sunlight (and
472 vice versa) can be common in sandy sediments during low tide (Hamels et al. 1998). Given the
473 prolonged harsh light conditions in these sediments, epipsammic diatoms probably demonstrate a
474 high de novo synthesis of photoprotective xanthophylls in situ, including Zx. This can also explain
475 the previously observed discrepancy between high Zx content and absence of colonial
476 cyanobacteria (containing Zx) in sandy sediments, as reported in Hamels et al. (1998). Taken
477 together, our results suggest that epipsammic diatoms use a combination of distinct photoprotective
478 strategies described by Lavaud and Lepetit (2013) to cope with the light climate of sandy intertidal
479 sediments: (1) a strong and fast reversible qE to track light fluctuations, combined with (2) high de
480 novo synthesis of de-epoxidized xanthophylls, probably unbound to the LHC antenna system,
481 which may fulfil an anti-oxidant function during prolonged light conditions. Even though our study

was performed on only one epipsammic representative, a strong qE and a relatively higher XC pool (compared to epipelic species) seem to be general for epipsammic species (Barnett et al. 2015).

The epipelic model *S. robusta* displayed a lower NPQ consisting partly of photoinhibition (qI). This is expected as epipelic diatoms use vertical migration and/or microcycling as their primary photoprotection mechanism when motility is allowed (Kromkamp et al. 1998; Serôdio 2004; Perkins et al. 2010; Cartaxana et al. 2011; Serôdio et al. 2012; Laviale et al. 2015). Furthermore, vertical migration is fast enough to reduce the amount of absorbed photons and can operate simultaneously with NPQ induction (Laviale et al. 2016). Both synthesis of new Dtx pigments and LHCX proteins, nonetheless, have been shown in epipelic communities under high light conditions (Laviale et al. 2015), which is in line with our findings. Furthermore, our data suggests the involvement of light-regulated LHCX proteins during harsh light conditions, allowing epipelic species to acclimate to prolonged higher light conditions (Ezequiel et al. 2015; Barnett et al. 2015). Hence, although adapted to a habitat with more cohesive sediments, characterized by a strongly attenuated photic zone (Cartaxana et al. 2016b), epipelic diatoms still possess the ability to increase their low basal photoprotective ability. The fact that epipelic species have been shown to emerge at the sediment surface at different times during tidal emersion suggests that they have different species-specific light niches (Paterson 1986; Underwood et al. 2005). As a result, their capacity for physiological photoprotection is also expected to differ between species. Future studies, therefore, should focus on the interspecific differences in the balance between behavioural and physiological photoprotection.

References

Armbrust, E. V. 2009. The life of diatoms in the world's oceans. Nature **459**: 185–92. doi:10.1038/nature08057

Bailleul, B., A. Rogato, A. de Martino, S. Coesel, P. Cardol, C. Bowler, A. Falciatore, and G. Finazzi. 2010. An atypical member of the light-harvesting complex stress-related protein family modulates diatom responses to light. Proc. Natl. Acad. Sci. **107**: 18214–18219. doi:10.1073/pnas.1007703107

Barnett, A., V. Méléder, L. Blommaert, and others. 2015. Growth form defines physiological photoprotective capacity in intertidal benthic diatoms. ISME J. **9**: 32–45. doi:10.1038/ismej.2014.105

Bonente, G., M. Ballottari, T. B. Truong, T. Morosinotto, T. K. Ahn, G. R. Fleming, K. K. Niyogi, and R. Bassi. 2011. Analysis of LhcSR3, a protein essential for feedback de-excitation in the green alga Chlamydomonas reinhardtii. T. Shikanai [ed.]. PLoS Biol. **9**: e1000577. doi:10.1371/journal.pbio.1000577

Brunet, C., and J. Lavaud. 2010. Can the xanthophyll cycle help extract the essence of the microalgal functional response to a variable light environment? J. Plankton Res. **32**: 1609–1617. doi:10.1093/plankt/fbq104

Cartaxana, P., S. Cruz, C. Gameiro, and M. Kühl. 2016a. Regulation of intertidal microphytobenthos photosynthesis over a diel emersion period is strongly affected by diatom migration patterns. Front. Microbiol. **7**: 872. doi:10.3389/fmicb.2016.00872

Cartaxana, P., L. Ribeiro, J. Goessling, S. Cruz, and M. Kühl. 2016b. Light and O2 microenvironments in two contrasting diatom-dominated coastal sediments. Mar. Ecol. Prog. Ser. **545**: 35–47. doi:10.3354/meps11630

Cartaxana, P., M. Ruivo, C. Hubas, I. Davidson, J. Serôdio, and B. Jesus. 2011. Physiological versus behavioral photoprotection in intertidal epipelic and epipsammic benthic diatom communities. J. Exp. Mar. Bio. Ecol. **405**: 120–127. doi:10.1016/j.jembe.2011.05.027

Consalvey, M., D. M. Paterson, and G. J. C. Underwood. 2004. The ups and downs of life in a benthic biofilm: Migration of benthic diatoms. Diatom Res. **19**: 181–202.

Dambek, M., U. Eilers, J. Breitenbach, S. Steiger, C. Büchel, and G. Sandmann. 2012. Biosynthesis of fucoxanthin and diadinoxanthin and function of initial pathway genes in Phaeodactylum tricornutum. J. Exp. Bot. **63**: 5607–5612. doi:10.1093/jxb/ers211

Dimier, C., F. Corato, F. Tramontano, and C. Brunet. 2007. Photoprotection and xanthophyll cycle activity in three marine diatoms. J. Phycol. **43**: 937–947. doi:10.1111/j.1529-8817.2007.00381.x

Domingues, N., A. R. Matos, J. Marques da Silva, and P. Cartaxana. 2012. Response of the diatom Phaeodactylum tricornutum to photooxidative stress resulting from high light exposure. PLoS One **7**: e38162. doi:10.1371/journal.pone.0038162

Ezequiel, J., M. Laviale, S. Frankenbach, P. Cartaxana, and J. Serôdio. 2015. Photoacclimation

state determines the photobehaviour of motile microalgae: The case of a benthic diatom. J. Exp. Mar. Bio. Ecol. **468**: 11–20. doi:10.1016/j.jembe.2015.03.004

Goss, R., and T. Jakob. 2010. Regulation and function of xanthophyll cycle-dependent photoprotection in algae. Photosynth. Res. **106**: 103–122. doi:10.1007/s11120-010-9536-x

Goss, R., and B. Lepetit. 2015. Biodiversity of NPQ. J. Plant Physiol. **172**: 13–32. doi:10.1016/j.jplph.2014.03.004

Goss, R., B. Lepetit, and C. Wilhelm. 2006a. Evidence for a rebinding of antheraxanthin to the light-harvesting complex during the epoxidation reaction of the violaxanthin cycle. J. Plant Physiol. **163**: 585–590. doi:10.1016/j.jplph.2005.07.009

Goss, R., E. A. Pinto, C. Wilhelm, and M. Richter. 2006b. The importance of a highly active and ΔpH-regulated diatoxanthin epoxidase for the regulation of the PS II antenna function in diadinoxanthin cycle containing algae. J. Plant Physiol. **163**: 1008–1021. doi:10.1016/j.jplph.2005.09.008

Hamels, I., K. Sabbe, K. Muylaert, C. Lucas, P. Herman, and W. Vyverman. 1998. Organisation of Microbenthic Communities. Eur. J. Protistol. **34**: 308–320.

Havaux, M., L. Dall'osto, and R. Bassi. 2007. Zeaxanthin has enhanced antioxidant capacity with respect to all other xanthophylls in Arabidopsis leaves and functions independent of binding to PSII antennae. Plant Physiol. **145**: 1506–1520. doi:10.1104/pp.107.108480

Havaux, M., and W. I. Gruszecki. 1993. Heat and light induced chlorophull a fluorescence changes in potato leaves containign high or low levels of the carotenoid zeaxanthin: indications of a regulatory effect of zeaxanthin on thylakoid fluidity. Photochem. Photobiol. **58**: 607–614. doi:10.1111/j.1751-1097.1993.tb04940.x

Van Heukelem, L., and C. S. Thomas. 2001. f phytoplankton pigments. J. Chromatogr. A **910**: 31–49.

Horton, P., and A. Hague. 1988. Studies on the induction of chlorophyll fluorescence in isolated barley protoplasts. IV. Resolution of non - photochemical quenching. Biochim. Biophys. Acta **932**: 107–115.

Jahns, P., D. Latowski, and K. Strzalka. 2009. Mechanism and regulation of the violaxanthin cycle: the role of antenna proteins and membrane lipids. Biochim. Biophys. Acta **1787**: 3–14. doi:10.1016/j.bbabio.2008.09.013

Janknegt, P. J., C. M. De Graaff, W. H. Van De Poll, R. J. W. Visser, E. W. Helbling, and A. G. J. Buma. 2009a. Antioxidative responses of two marine microalgae during acclimation to static and fluctuating natural uv radiation. Photochem. Photobiol. **85**: 1336–1345. doi:10.1111/j.1751-1097.2009.00603.x

Janknegt, P. J., C. M. De Graaff, W. H. Van De Poll, R. J. W. Visser, J. W. Rijstenbil, and A. G. J. Buma. 2009b. Short-term antioxidative responses of 15 microalgae exposed to excessive irradiance including ultraviolet radiation. Eur. J. Phycol. **44**: 525–539. doi:10.1080/09670260902943273

Janknegt, P. J., W. H. van de Poll, R. J. W. Visser, J. W. Rijstenbil, and A. G. J. Buma. 2008. Oxidative Stress Responses in the Marine Antarctic Diatom Chaetoceros Brevis (Bacillariophyceae) During Photoacclimation 1. J. Phycol. **44**: 957–966. doi:10.1111/j.1529-8817.2008.00553.x

Jeffrey, S. W., and G. S. Humphrey. 1975. New spectrophotometric equations for determining chlorophylls a, b, c1 and c2 in higher plants, algae and natural phytoplankton. Biochem Physiol Pflanz. Bd **167**: 191–194.

Jesus, B., V. Brotas, L. Ribeiro, C. R. Mendes, P. Cartaxana, and D. M. Paterson. 2009. Adaptations of microphytobenthos assemblages to sediment type and tidal position. Cont. Shelf Res. **29**: 1624–1634. doi:10.1016/j.csr.2009.05.006

Juneau, P., A. Barnett, V. Méléder, C. Dupuy, and J. Lavaud. 2015. Combined effect of high light and high salinity on the regulation of photosynthesis in three diatom species belonging to the main growth forms of intertidal flat inhabiting microphytobenthos. J. Exp. Mar. Bio. Ecol. **463**: 95–104. doi:10.1016/j.jembe.2014.11.003

Kromkamp, J. C., C. Barranguet, and J. Peene. 1998. Determination of microphytobenthos PSII quantum efficiency and photosynthetic activity by means of variable chlorophyll fluorescence. Mar. Ecol. Prog. Ser.

Kuhl, M., C. Lassen, and B. B. Jorgensen. 1994. Light penetration and light intensity in sandy marine sediments measured with irradiance and scalar irradiance fiber-optic microprobes. Mar. Ecol. Prog. Ser. **105**: 139–148. doi:10.3354/meps105139

Lavaud, J., and R. Goss. 2014. The peculiar features of the non-photochemical fluorescence quenching in diatoms and brown algae, p. 421–443. *In* Non-Photochemical Quenching and Energy Dissipation in Plants, Algae and Cyanobacteria. Springer.

Lavaud, J., and B. Lepetit. 2013. An explanation for the inter-species variability of the photoprotective non-photochemical chlorophyll fluorescence quenching in diatoms. Biochim. Biophys. Acta **1827**: 294–302. doi:10.1016/j.bbabio.2012.11.012

Lavaud, J., B. Rousseau, and A.-L. Etienne. 2004. General Features of Photoprotection By Energy Dissipation in Planktonic Diatoms (Bacillariophyceae). J. Phycol. **40**: 130–137. doi:10.1046/j.1529-8817.2004.03026.x

Lavaud, J., C. Six, and D. A. Campbell. 2016. Photosystem II repair in marine diatoms with contrasting photophysiologies. Photosynth. Res. **127**: 189–199. doi:10.1007/s11120-015-0172-3

Lavaud, J., R. F. Strzepek, and P. G. Kroth. 2007. Photoprotection capacity differs among diatoms : Possible consequences on the spatial distribution of diatoms related to fluctuations in the underwater light climate. Limnol. Oceanogr. **52**: 1188–1194.

Laviale, M., A. Barnett, J. Ezequiel, B. Lepetit, S. Frankenbach, V. Méléder, J. Serôdio, and J. Lavaud. 2015. Response of intertidal benthic microalgal biofilms to a coupled light-temperature stress: evidence for latitudinal adaptation along the Atlantic coast of Southern Europe. Environ. Microbiol. **17**: 3662–3677. doi:10.1111/1462-2920.12728

618 Laviale, M., S. Frankenbach, and J. Serôdio. 2016. The importance of being fast: comparative
619 kinetics of vertical migration and non-photochemical quenching of benthic diatoms under
620 light stress. Mar. Biol. **163**: 10. doi:10.1007/s00227-015-2793-7

621 Lepetit, B., G. Gélin, M. Lepetit, and others. *In press*. The diatom Phaeodactylum tricornutum
622 adjusts nonphotochemical fluorescence quenching capacity in response to dynamic light via
623 fine-tuned Lhcx and xanthophyll cycle pigment synthesis. New Phytol.
624 doi:10.1111/nph.14337

625 Lepetit, B., S. Sturm, A. Rogato, A. Gruber, M. Sachse, A. Falciatore, P. G. Kroth, and J.
626 Lavaud. 2013. High light acclimation in the secondary plastids containing diatom
627 Phaeodactylum tricornutum is triggered by the redox state of the plastoquinone pool. Plant
628 Physiol. **161**: 853–865. doi:10.1104/pp.112.207811

629 Lepetit, B., D. Volke, M. Gilbert, C. Wilhelm, and R. Goss. 2010. Evidence for the existence of
630 one antenna-associated, lipid-dissolved and two protein-bound pools of diadinoxanthin cycle
631 pigments in diatoms. Plant Physiol. **154**: 1905–1920. doi:10.1104/pp.110.166454

632 Lohr, M., and C. Wilhelm. 1999. Algae displaying the diadinoxanthin cycle also possess the
633 violaxanthin cycle. Proc. Natl. Acad. Sci. **96**: 8784–8789.

634 Lohr, M., and C. Wilhelm. 2001. Xanthophyll synthesis in diatoms: quantification of putative
635 intermediates and comparison of pigment conversion kinetics with rate constants derived
636 from a model. Planta **212**: 382–391. doi:10.1007/s004250000403

637 MacIntyre, H. L., T. M. Kana, T. Anning, and R. J. Geider. 2002. Photoacclimation of
638 photosynthesis irradiance response curves and photosynthetic pigments in macroalgae and
639 cyanobacteria. J. Phycol. **38**: 17–38. doi:10.1046/j.1529-8817.2002.00094.x

640 Nymark, M., K. C. Valle, T. Brembu, K. Hancke, P. Winge, K. Andresen, G. Johnsen, and A. M.
641 Bones. 2009. An integrated analysis of molecular acclimation to high light in the marine
642 diatom Phaeodactylum tricornutum. PLoS One **4**: e7743. doi:10.1371/journal.pone.0007743

643 Owens, T. G. 1986. Light-Harvesting Function in the Diatom Phaeodactylum tricornutum II.
644 distribution of excitation energy between photosystems. **80**: 739–746.

645 Park, S., G. Jung, Y. Hwang, and E. Jin. 2010. Dynamic response of the transcriptome of a
646 psychrophilic diatom, Chaetoceros neogracile, to high irradiance. Planta **231**: 349–60.
647 doi:10.1007/s00425-009-1044-x

648 Paterson, D. M. 1986. The migratory behaviour of diatom assemblages in a laboratory tidal
649 micro-ecosystem examined by low temperature scanning electron microscopy. Diatom Res.
650 **1**: 227–239. doi:10.1080/0269249X.1986.9704971

651 Perkins, R. G., J. C. Kromkamp, J. Serôdio, J. Lavaud, B. Jesus, J. L. Mouget, S. Lefebvre, and
652 R. M. Forster. 2011. The application of variable chlorophyll fluorescence to
653 microphytobenthic biofilms, p. 237–275. *In* Chlorophyll a Fluorescence in Aquatic
654 Sciences: Methods and Applications. Springer Netherlands.

655 Perkins, R., J. Lavaud, J. Serôdio, and others. 2010. Vertical cell movement is a primary response

of intertidal benthic biofilms to increasing light dose. Mar. Ecol. Prog. Ser. **416**: 93–103. doi:10.3354/meps08787

Petrou, K., M. A. Doblin, and P. J. Ralph. 2011. Heterogeneity in the photoprotective capacity of three Antarctic diatoms during short-term changes in salinity and temperature. Mar. Biol. **158**: 1029–1041. doi:10.1007/s00227-011-1628-4

Pniewski, F. F., P. Biskup, I. Bubak, P. Richard, A. Latała, and G. Blanchard. 2015. Photo-regulation in microphytobenthos from intertidal mudflats and non-tidal coastal shallows. Estuar. Coast. Shelf Sci. **152**: 153–161. doi:10.1016/j.ecss.2014.11.022

Ribeiro, L., V. Brotas, Y. Rincé, and B. Jesus. 2013. Structure and diversity of intertidal benthic diatom assemblages in contrasting shores: a case study from the Tagus estuary. J. Phycol. **49**: 258–270. doi:10.1111/jpy.12031

Schumann, A., R. Goss, T. Jakob, and C. Wilhelm. 2007. Investigation of the quenching efficiency of diatoxanthin in cells of Phaeodactylum tricornutum (Bacillariophyceae) with different pool sizes of xanthophyll cycle pigments. Phycologia **46**: 113–117. doi:10.2216/06-30.1

Serôdio, J. 2004. Analysis of variable chlorophyll fluorescence in microphytobenthos assemblages: implications of the use of depth-integrated measurements. Aquat. Microb. Ecol. **36**: 137–152. doi:10.3354/ame036137

Serôdio, J., J. Ezequiel, A. Barnett, J. Mouget, V. Méléder, M. Laviale, and J. Lavaud. 2012. Efficiency of photoprotection in microphytobenthos: role of vertical migration and the xanthophyll cycle against photoinhibition. Aquat. Microb. Ecol. **67**: 161–175. doi:10.3354/ame01591

Su, W., T. Jakob, and C. Wilhelm. 2012. the Impact of Nonphotochemical Quenching of Fluorescence on the Photon Balance in Diatoms Under Dynamic Light Conditions. J. Phycol. **48**: 336–346. doi:10.1111/j.1529-8817.2012.01128.x

Taddei, L., G. R. Stella, A. Rogato, and others. 2016. Multisignal control of expression of the LHCX protein family in the marine diatom Phaeodactylum tricornutum. J. Exp. Bot. **67**: 3939–3951. doi:10.1093/jxb/erw198

Underwood, G. J. C., and J. Kromkamp. 1999. Primary production by phytoplankton and microphytobenthos in estuaries estuaries. Adv. Ecol. Res. **29**: 93–153. doi:10.1016/S0065-2504(08)60192-0

Underwood, G. J. C., R. G. Perkins, M. C. Consalvey, A. R. M. Hanlon, K. Oxborough, N. R. Baker, and D. M. Paterson. 2005. Patterns in microphytobenthic primary productivity: Species-specific variation in migratory rhythms and photosynthesis in mixed-species biofilms. Limnol. Oceanogr. **50**: 755–767. doi:10.4319/lo.2005.50.3.0755

Wagner, H., T. Jakob, J. Lavaud, and C. Wilhelm. 2016. Photosystem II cycle activity and alternative electron transport in the diatom Phaeodactylum tricornutum under dynamic light conditions and nitrogen limitation. Photosynth. Res. **128**: 151–161.

694 Waring, J., M. Klenell, U. Bechtold, G. J. C. Underwood, and N. R. Baker. 2010. Light-Induced
695 Responses of Oxygen Photoreduction, Reactive Oxygen Species Production and Scavenging
696 in Two Diatom Species. J. Phycol. **46**: 1206–1217. doi:10.1111/j.1529-8817.2010.00919.x

697 Westermann, M., and E. Rhiel. 2005. Localisation of fucoxanthin chlorophyll a/c-binding
698 polypeptides of the centric diatom Cyclotella cryptica by immuno-electron microscopy.
699 Protoplasma **225**: 217–223. doi:10.1007/s00709-005-0083-9

700 Wu, H., A. M. Cockshutt, A. McCarthy, and D. a Campbell. 2011. Distinctive photosystem II
701 photoinactivation and protein dynamics in marine diatoms. Plant Physiol. **156**: 2184–95.
702 doi:10.1104/pp.111.178772

703 Zhu, S.-H., and B. R. Green. 2010. Photoprotection in the diatom Thalassiosira pseudonana: role
704 of LI818-like proteins in response to high light stress. Biochim. Biophys. Acta **1797**: 1449–
705 57. doi:10.1016/j.bbabio.2010.04.003

706

707

Acknowledgements

The authors would like to thank the Research Foundation Flanders (FWO project G.0222.09N), Ghent University (BOF-GOA 01G01911) and the Egide/Campus France-PHC Tournesol (n128992UA) exchange program for their financial support. JL also thanks the CNRS and the French consortium CPER Littoral for their financial support. M.J.J.H. acknowledges a Postdoctoral Fellowship of the Research Foundation Flanders.

Figure legends

Fig. 1a&b Photophysiological measurements

O. guenter-grassii (filled circles) and *S. robusta* (open circles) were exposed to one hour of HL (2000 µM photons m^{-2} s^{-1}) and one subsequent hour of recovery in low light (LL, 20 µM photons m^{-2} s^{-1}). The quantum yield of PSII ($\Delta F/F_m'$) **(a)**, expressed in percentage of the maximal photosynthetic efficiency of PSII (F_v/F_m) before HL exposure and **(b)** Non-photochemical quenching (NPQ). Values represent averages of three independent measurements ± standard deviations.

Fig. 2 Dark recovery of *O. guenter-grassii* after HL exposure

O. guenter-grassii was exposed to one hour of HL (2000 µM photons m^{-2} s^{-1}) and one subsequent hour of recovery in low light (LL, 20 µM photons m^{-2} s^{-1})(filled circles) or in dark recovery (open circles) with LL onset at 105 min (indicated by an arrow). **(a)** Photosynthetic efficiency of PSII $\Delta F/F_m'$ is expressed in percentage of the maximal photosynthetic efficiency of PSII (F_v/F_m) measured before high light onset. **(b)** Non-photochemical quenching (NPQ) and **(c)** Dtx, expressed in mol (100 mol Chl *a*)$^{-1}$. Values represent averages of three independent measurements ± standard deviations for the low light recovery treatment. For the dark recovery treatment, only one replicate is plotted.

Fig. 3a,b,c&d Xanthophyll cycle kinetics

O. guenter-grassii and *S. robusta* were exposed to one hour of HL (2000 µM photons m^{-2} s^{-1}) and one subsequent hour of recovery in low light (LL, 20 µM photons m^{-2} s^{-1}). **(a)** Diadinoxanthin

cycle kinetics of *O. guenter-grassii;* **(b)** Diadinoxanthin cycle kinetics of *S. robusta*; **(c)** Violaxanthin cycle kinetics of *O. guenter-grassii*; **(d)** Violaxanthin cycle kinetics of *S. robusta*. Short dashed lines represent the epoxidized pigment (Ddx or Vx) whereas solid lines represent the fully de-epoxidized pigment (Dtx of Zx). The grey line represents the intermediate Ax. Long dashed lines represent the sum of all xanthophylls per cycle. Values represent averages of three independent measurements ± standard deviations.

Fig. 4 De-epoxidation state of *O. guenter-grassii* and *S. robusta*

O. guenter-grassii (filled circles) and *S. robusta* (open circles) were exposed to one hour of HL (2000 µM photons m^{-2} s^{-1}) and one subsequent hour of recovery in low light (LL, 20 µM photons m^{-2} s^{-1}). De-epoxidation state (DES) was calculated as 100[Dtx/(Ddx + Dtx)].

Fig. 5a&b Relationship between NPQ and Dtx

NPQ is plotted in function of Dtx, sampled at the same timepoints for *O. guenter-grassii* **(a, circles)** and *S. robusta* **(b, triangles)**, exposed to one hour of HL (2000 µM photons m^{-2} s^{-1}) and one subsesquent hour of recovery in low light (LL, 20 µM photons m^{-2} s^{-1}). White symbols represent data points sampled during HL, whereas black symbols represent data points sampled during LL recovery. For *O. guenter-grassii* a distinction is made in the relationship below (solid line, slope $p < 0.001$) and above 3 mol Dtx (100 mol Chl *a*)$^{-1}$ (dashed line, slope $p < 0.001$). The NPQ/Dtx relationship for *S. robusta* is represented by a dotted line (slope $p < 0.001$, intercept $p < 0.001$).

Fig. 6a&b Western blot of LHCX proteins

Western blot of **(a)** *O. guenter-grassii* using an FCP6 antibody and **(b)** *S. robusta* using anti-LHCSR3 sampled before (T0) exposure to HL (2000 µM photons m^{-2} s^{-1}), after one hour of HL

(HL) and after one subsequent hour of recovery in LL (20 μM photons m^{-2} s^{-1}) (HL + LL). An antibody against the plastid encoded PsbB (CP47) protein was used as a loading control. *Phaeodactylum tricornutum* (P.t.) samples which were exposed to HL for 3 hours were analysed at the same time as a control. *Phaeodactylum* samples showed three LHCX bands using the LHCSR3 antibody which were previously identified as LHCX1, LHCX2 and LHCX3 (Lepetit et al., 2013). Identification of P.t. LHCX2&3 was less clear using the FCP6 antibody in (a).

765 # Tables

766

	S. robusta	*O. guenter-grassii*
Ddx + Dtx content [mol (100 Chl *a*)$^{-1}$]	**4.942** ±0.479	**9.880** ±0.594
Dtx after 60 min HL [mol (100 Chl *a*)$^{-1}$]	**3.146** ±0.424	**5.685** ±1.413
Ddx deepoxidaton rate [min^{-1}]	**0.081** ±0.017	**0.164** ±0.0521
De novo synthetized Dtx [mol (100 Chl *a*)$^{-1}$]	**1.976** ±0.422	**2.138** ±0.612
Dtx de novo synthesis rate [mmol (mol Chl *a*)$^{-1}$ min^{-1}]	**0.341** ±0.035	**0.444** ±0.065
De novo synthetized Vx cycle pigments [mol (100 Chl *a*)$^{-1}$]	**0.131** ±0.010	**2.043** ±0.216
De novo synthesis rate Vx cycle pigments [mmol (mol Chl *a*)$^{-1}$ min^{-1}]	**0.0185** ±0.009	**0.35** ±0.025
Dtx epoxidation rate in LL [min^{-1}]	**0.08** ±0.01	**0.406** ±0.144
Zx epoxidation rate in LL [min^{-1}]	**n.d.**	**0.311** ±0.060

767

768 **Table 1 Xanthophyll cycle characteristics**

Abbreviations: Chl *a*, Chlorophyll *a*; Ddx, diadinoxanthin; Dtx, diatoxanthin; Vx, violaxanthin; Zx, zeaxanthin. All pigments are expressed as mol (100 mol chlorophyll *a*)$^{-1}$. Epoxidation and de-epoxidation rates are calculated by fitting exponential decay functions. De novo synthesis rates were fitted with linear functions. Values represent averages of three independent measurements ± standard deviations.

Figures

Fig. 1a&b

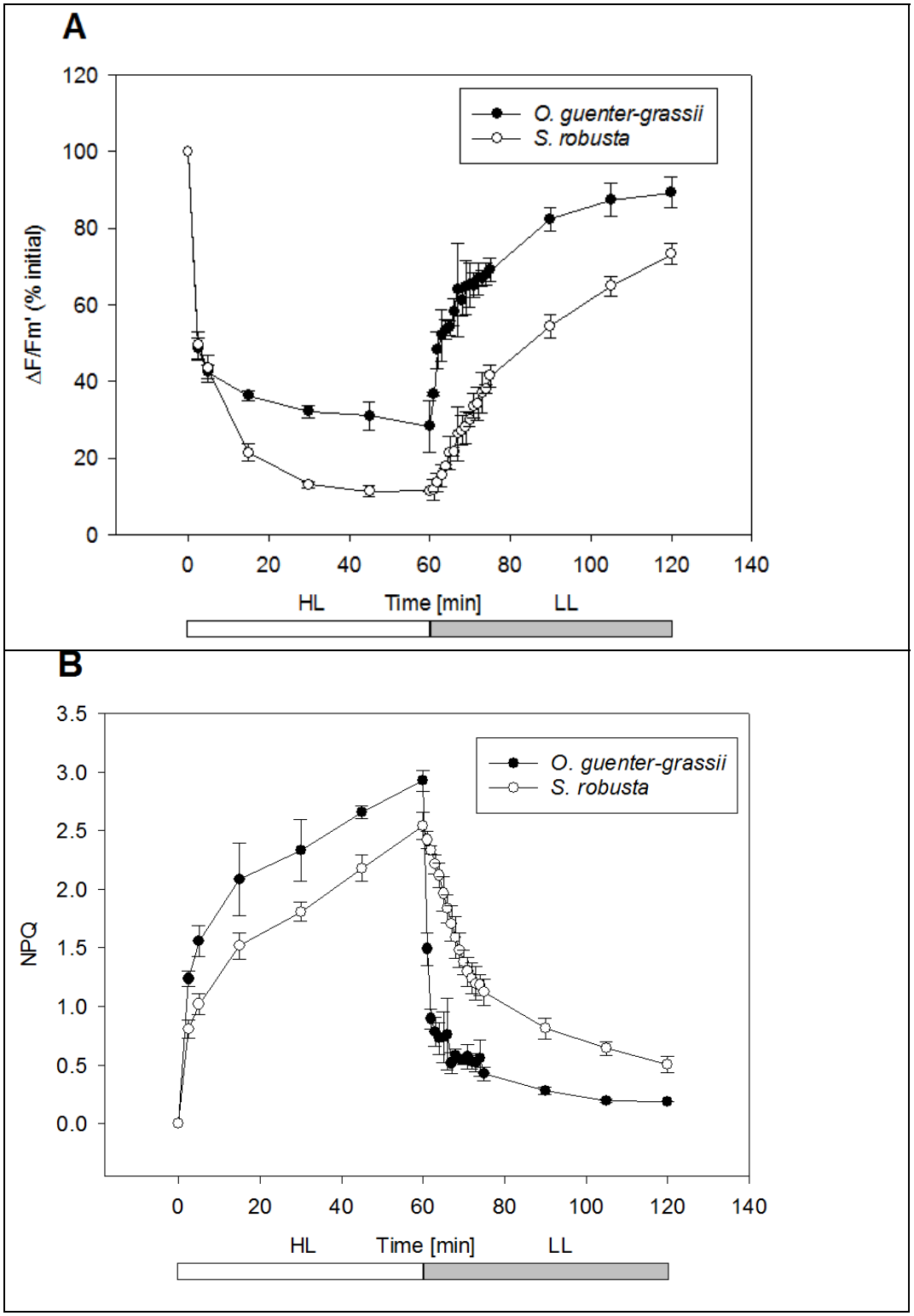

802 **Fig 2a,b,c&d**

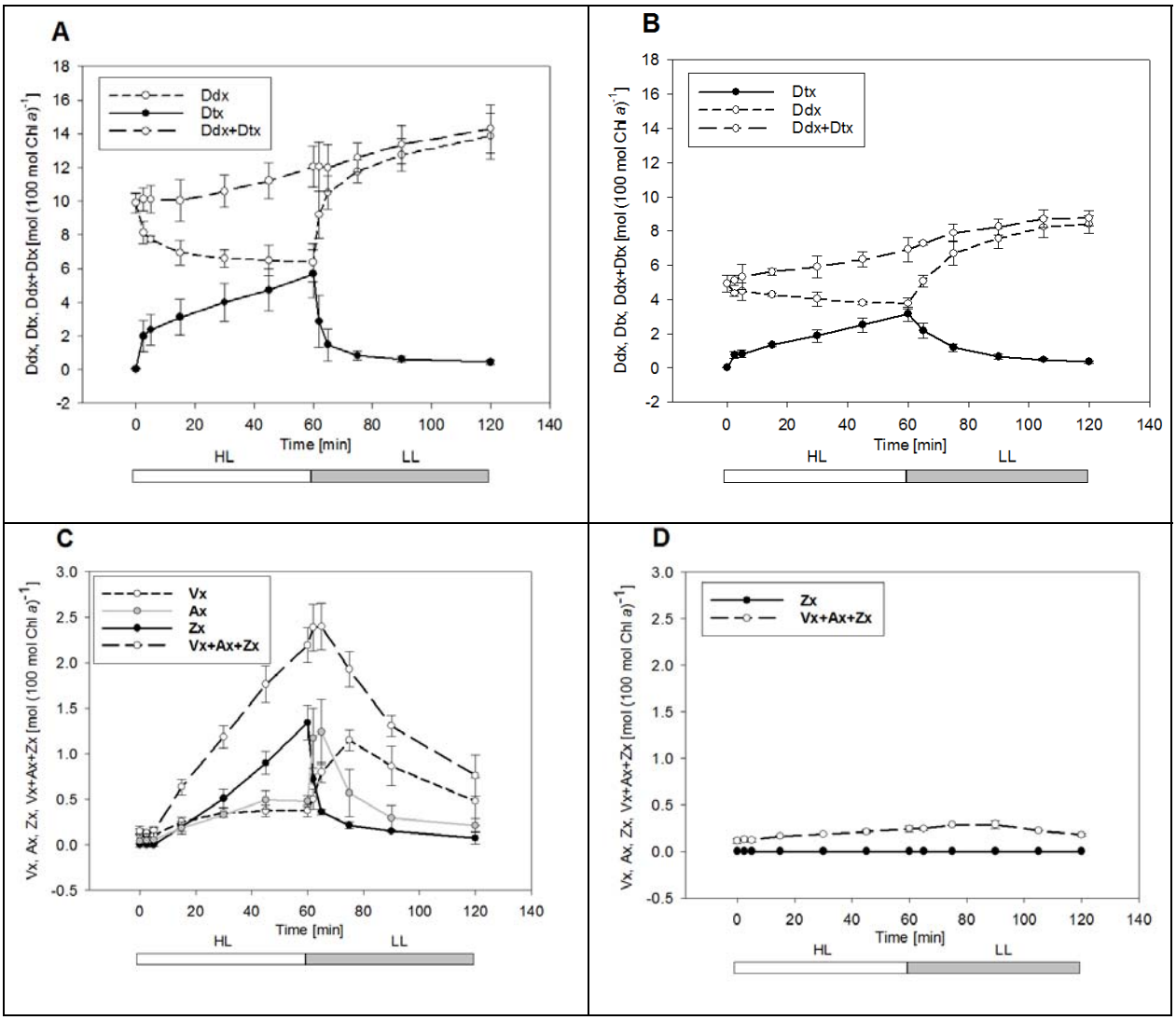

803

804

805

806 **Fig. 3a&b**

807

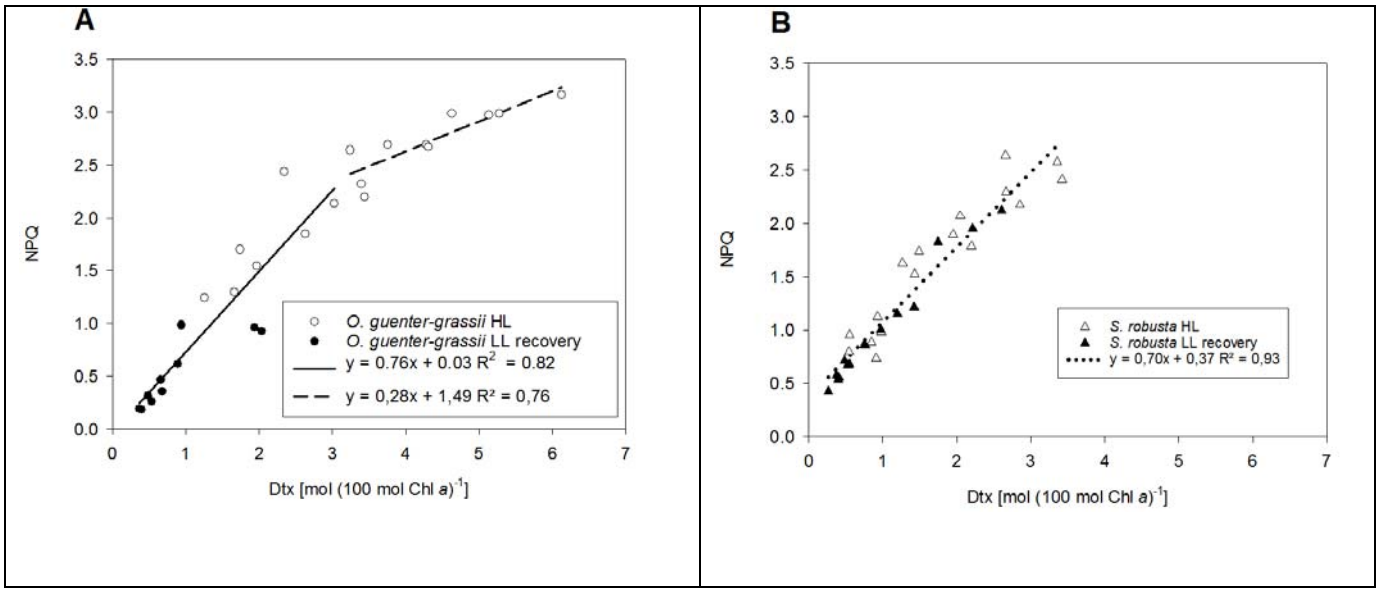

808

809 **Fig. 4a&b**

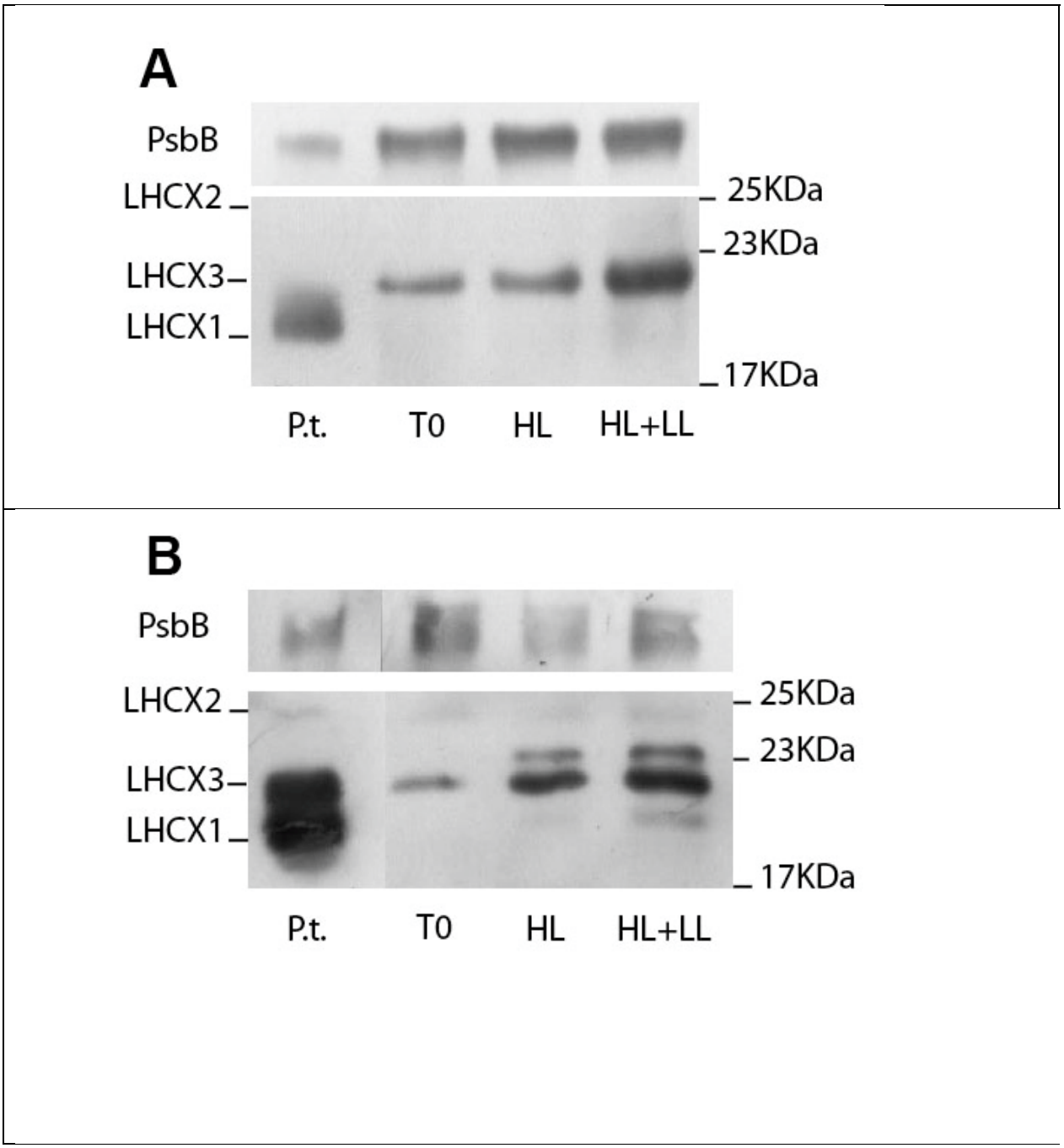

810

811

812

Supporting material

Fig. S1a,b&c

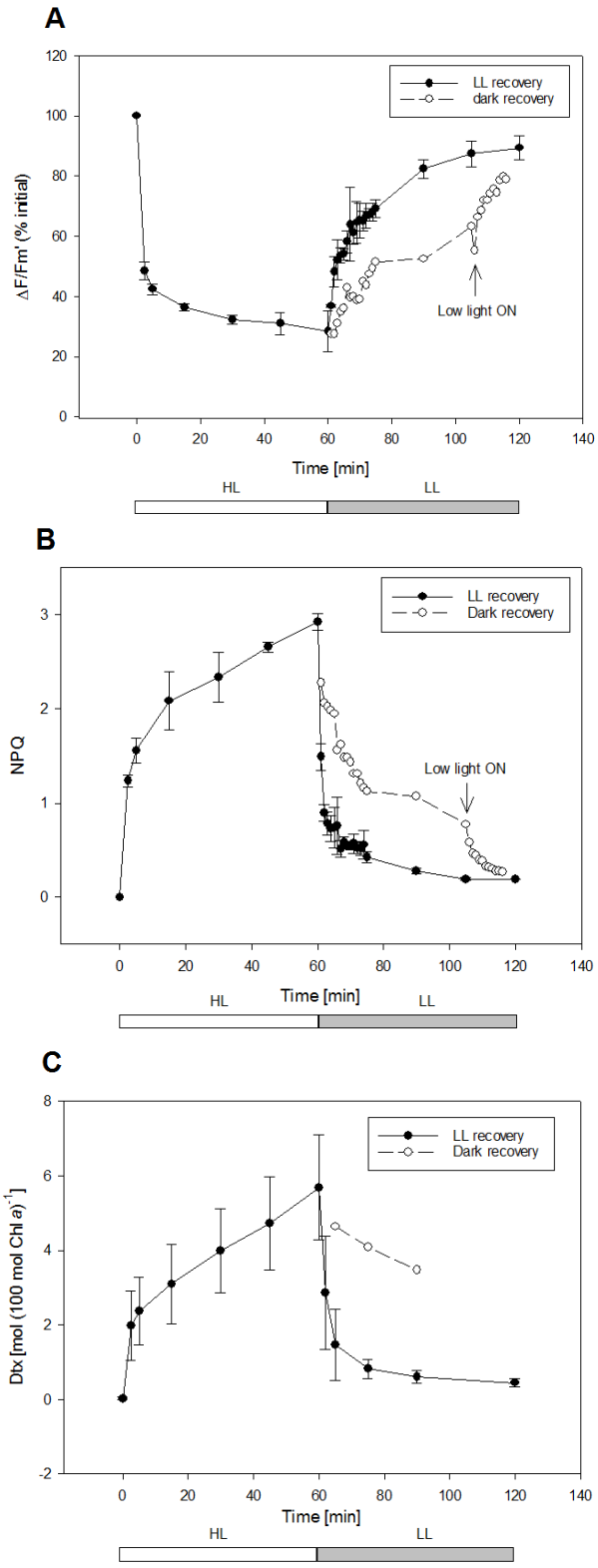

Fig. S1a,b&c Dark recovery of *O. guenter-grassii* after HL exposure

O. guenter-grassii was exposed to one hour of HL (2000 µM photons m^{-2} s^{-1}) and one subsequent hour of recovery in low light (LL, 20 µM photons m^{-2} s^{-1})(filled circles) or in dark recovery (open circles) with LL onset at 105 min (indicated by an arrow). **(a)** Photosynthetic efficiency of PSII ΔF/Fm' is expressed in percentage of the maximal photosynthetic efficiency of PSII (Fv/Fm) measured before high light onset. **(b)** Non-photochemical quenching (NPQ) and **(c)** Dtx, expressed in mol (100 mol Chl *a*)$^{-1}$. Values represent averages of three independent measurements ± standard deviations for the low light recovery treatment. For the dark recovery treatment, only one replicate is plotted.

826 **Fig. S2**

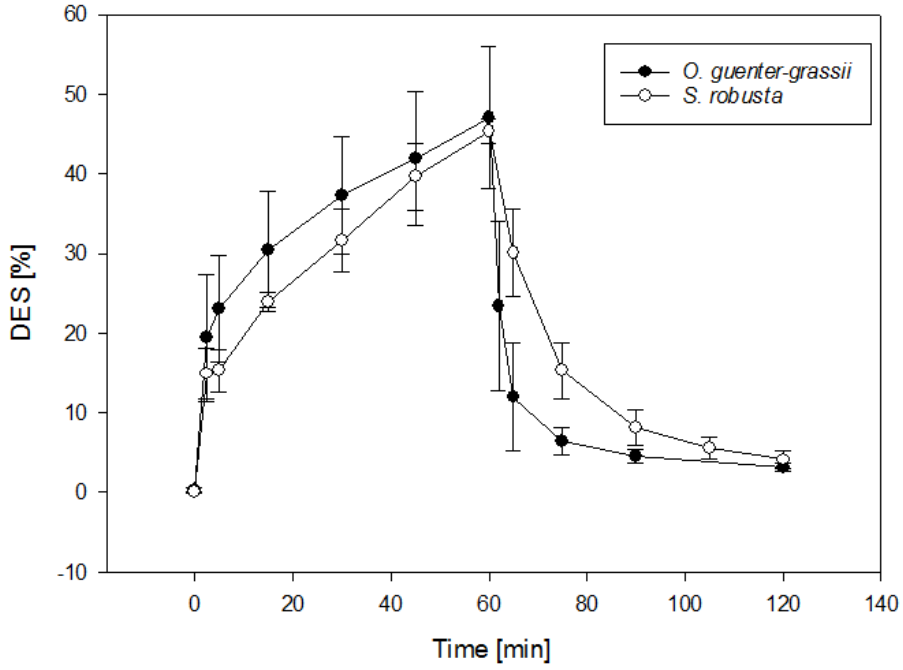

827

828 **Fig. S2 De-epoxidation state of *O. guenter-grassii* and *S. robusta***

829 *O. guenter-grassii* (filled circles) and *S. robusta* (open circles) were exposed to one hour of HL

830 (2000 µM photons m^{-2} s^{-1}) and one subsequent hour of recovery in low light (LL, 20 µM photons

831 m^{-2} s^{-1}). De-epoxidation state (DES) was calculated as 100[Dtx/(Ddx+Dtx)].

832

833 **Fig. S3a&b**

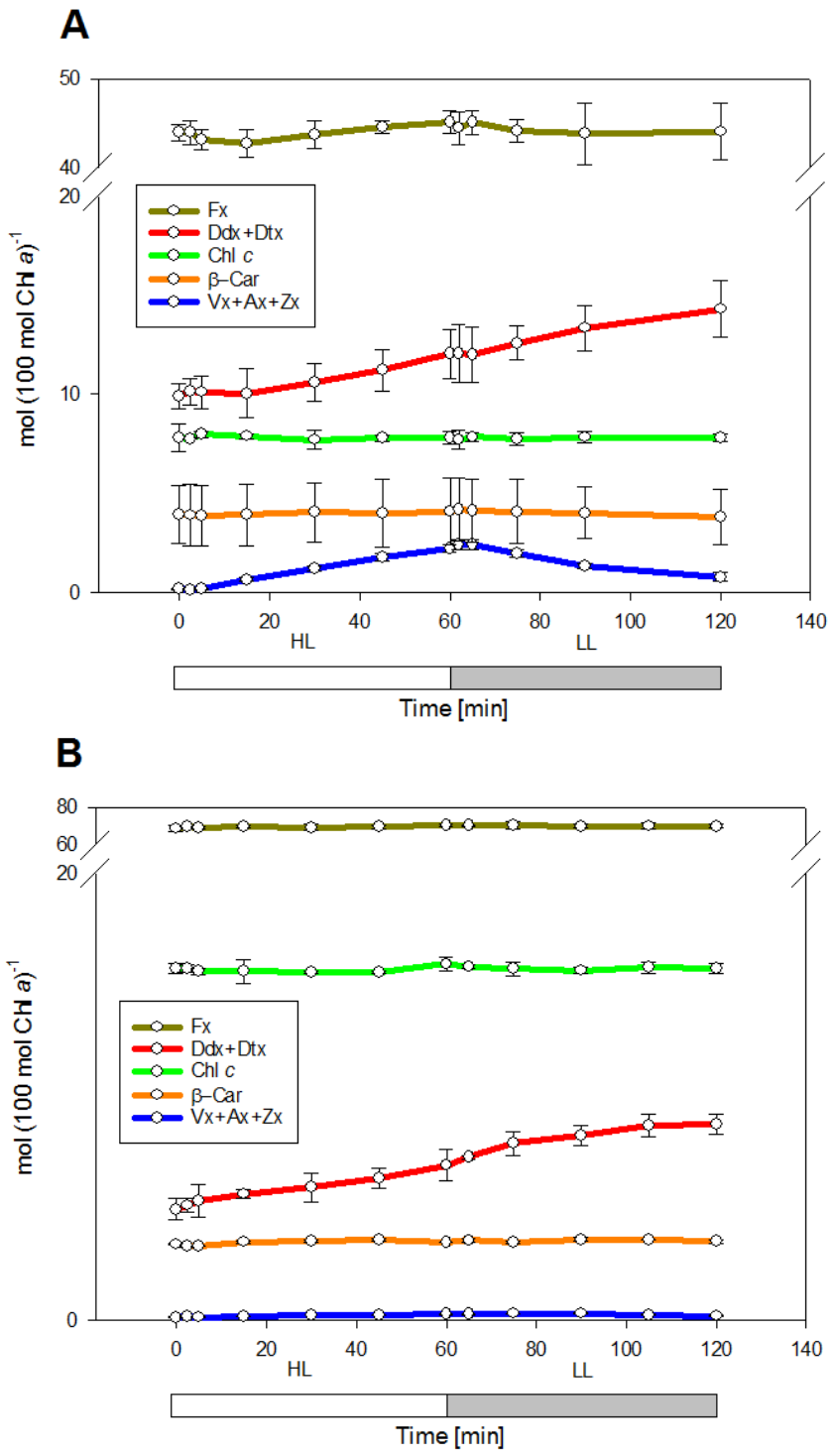

834

Fig. S3a&b

O. guenter-grassii and *S. robusta* were exposed to one hour of HL (2000 µM photons m^{-2} s^{-1}) and one subsequent hour of recovery in low light (LL, 20 µM photons m^{-2} s^{-1}). **(a)** Pigment kinetics in *O. guenter-grassii;* **(b)** Pigment kinetics in *S. robusta*. Abbreviations: Fx, fucoxanthin; Chl *c*, Chlorophyll *c*; Ddx, diadinoxanthin; Dtx, diatoxanthin; Vx, violaxanthin; Ax, antheraxanthin; Zx, zeaxanthin; *β*-car*, β*-carotene.